Microchim Acta (2015) 182:2131–2138
DOI 10.1007/s00604-015-1547-z

ORIGINAL PAPER

Colorimetric method for determination of bisphenol A based on aptamer-mediated aggregation of positively charged gold nanoparticles

Jingyue Xu[1] · Ying Li[1] · Jiaxin Bie[1] · Wei Jiang[2] · Jiajia Guo[1] · Yeli Luo[1] · Fei Shen[1] · Chunyan Sun[1]

Received: 2 April 2015 / Accepted: 15 June 2015 / Published online: 1 July 2015

Abstract A sensitive, specific and rapid colorimetric aptasensor for the determination of the plasticizer bisphenol A (BPA) was developed. It is based on the use of gold nanoparticles (AuNPs) that are positively charged due to the modification with cysteamine which is cationic at near-neutral pH values. If aptamers are added to such AuNPs, aggregation occurs due to electrostatic interactions between the negatively-charged aptamers and the positively-charged AuNPs. This results in a color change of the AuNPs from red to blue. If a sample containing BPA is added to the anti-BPA aptamers, the anti-BPA aptamers undergo folding via an induced-fit binding mechanism. This is accompanied by a conformational change, which prevents the aptamer-induced aggregation and color change of AuNPs. The effect was exploited to design a colorimetric assay for BPA. Under optimum conditions, the absorbance ratio of A_{527}/A_{680} is linearly proportional to the BPA concentration in the range from 35 to 140 ng mL^{-1}, with a detection limit of 0.11 ng mL^{-1}. The method has been successfully applied to the determination of BPA in spiked tap water and gave recoveries between 91 and 106 %. Data were in full accordance with results obtained from HPLC. This assay is selective, easily performed, and in our perception represents a promising alternative to existing methods for rapid quantification of BPA.

Keywords Bisphenol A · Aptamer · Colorimetry · Gold nanoparticles · Electrostatic interactions · Cysteamine

Introduction

Bisphenol A [BPA; 2,2-bis (4-hydroxyphenyl) propane] is commonly used in the manufacturing of polycarbonate plastics, epoxy resins, food contact ware like baby bottles, and protective coatings on food containers. Due to such widespread uses, human are widely exposed to significant amounts of BPA. As a known endocrine disruptor, BPA poses serious risks to human health, such as brain development, sexual activity, male fertility, diabetes and obesity [1]. BPA is banned for the use in baby bottles in many countries including China. Moreover, it is evidenced that BPA has contributed significantly to the environmental problem in the "low dose" range [2]. Thus, the detection of BPA in food and environment has captured extensive attention.

Nowadays, many techniques have been used to measure BPA, such as liquid chromatography-mass spectrometry (LC-MS) [3], high performance liquid chromatography (HPLC) [4] and gas chromatography-mass spectrometry (GC-MS) [2]. These methods are very sensitive and accurate, but they are time-consuming and need to be performed by well-trained technicians. Therefore, these techniques are unsuitable for on-line or field monitoring. Other methods like electrochemical sensor [5, 6] and enzyme linked immunosorbent assay (ELISA) [7] have also been reported for the determination of BPA. Electrochemical sensors are widely applied in detecting BPA based on the electroactivity of the phenolic

Jingyue Xu and Ying Li contributed equally to this work.

Electronic supplementary material The online version of this article (doi:10.1007/s00604-015-1547-z) contains supplementary material, which is available to authorized users.

✉ Chunyan Sun
sunchuny@jlu.edu.cn; sunchunyan1977@163.com

[1] Department of Food Quality and Safety, Jilin University, Changchun 130062, China

[2] Laboratory of Nutrition and Functional Food, Jilin University, Changchun 130062, China

groups in the BPA molecule, but generally with poor specificity and relatively low sensitivity. ELISA possesses the advantage of high sensitivity, but it has been reported that the ELISA method may give erroneous values due to non-specific binding to the antibody, leading to an overestimation of trace amounts of BPA concentration. Therefore, it is of great importance to establish a simple, sensitive and accurate method for the determination of BPA.

Aptamers are in-vitro selected single-stranded nucleic acids which are screened by the classic systematic evolution of ligands by exponential enrichment (SELEX) technique [8, 9]. Compared with antibodies, aptamers display the excellent advantages of small size, easier artificial synthesis and modification, cost-effectiveness, thermal stability, as well as chemical robustness. Particularly, aptamers possess high specific recognition ability towards a broader range of targets ranging from small inorganic and organic substances to proteins and even whole cells and bacteria [10–14]. The secondary structures of aptamers can be engineered to undergo analyte-dependent conformational changes, which opens up a wealth of possible signal transduction schemas, irrespective of whether the detection modality is optical, electrochemical, or mass based [15, 16]. Among them, colorimetry as the simplest sensing pattern has been widely developed for aptasensors, enabling color visualization without a specific instrument. Due to their high extinction coefficients and distance-dependent optical properties, gold nanoparticles (AuNPs) have shown tremendous potential in colorimetric aptasensors, based on the phenomenon that the appearance color of dispersed AuNPs in solution will change from red to blue after aggregation due to the shift of surface plasmon resonance to a higher wavelength. AuNPs-based aptasensors can be divided into two categories: DNA-functionalized AuNPs aptasensors and unfunctionalized AuNPs aptasensors. DNA-functionalized AuNPs aptasensors need the function of AuNPs with thiolated DNA, which is a time-consuming process (1–2 days). So, many unfunctionalized AuNPs-based aptasensors have been developed for a simple and rapid detection. In unfunctionalized AuNPs aptasensors, the unfolded aptamers can be adsorbed onto the negatively-charged AuNPs via the coordination interaction between the DNA nitrogen atoms and the AuNPs, thus prevent AuNPs from aggregating in salt solution. When aptamers turn into a target-aptamer complex, aptamers will be released from the AuNPs, so the addition of salt leads to the aggregation of AuNPs. Based on this principle, many metal ions [17], small molecules like BPA [18, 19], and proteins [20] have been detected using the negatively-charged AuNPs. However, the salt-induced assembly of AuNPs-based colorimetric detection is susceptible to the sensing environments (acidity, ionic strength, etc.) and can potentially suffer from false positive signal readouts. Moreover, the presence of indispensable salt solution makes the optimization and operation of this method more complicated.

It has been reported that positively-charged cysteamine-capped AuNPs (cysteamine-AuNPs) can serve as an excellent colorimetric probe for the rapid detection of enzyme activity and heparin [21–23]. Herein, we exploited the application of positively-charged AuNPs as the reporter in colorimetric aptasensors and have established a visual strategy for BPA monitoring. As shown in Scheme 1, the negatively-charged anti-BPA aptamers can absorb onto the positively-charged cysteamine-AuNPs via electrostatic interactions, which causes the aggregation of AuNPs accompanied with the rapid red-to-blue color change. In the presence of BPA, the specific binding of BPA with the aptamers induces the conformation changes of anti-BPA aptamers [24], which can release the aptamers from cysteamine-AuNPs and thus prevents the aggregation and color change of cysteamine-AuNPs. This provides the basis for our visual BPA detection method. The method was successfully applied to detect BPA in tap water samples with satisfactory results, which were further confirmed by HPLC. This colorimetric aptasensor for BPA is inexpensive, less time-consuming, easy to operate and would facilitate the on-site monitoring of BPA.

Experimental

Reagents

The synthetic anti-BPA aptamers (sequence designed by [25]), 5′-CCG GTG GGT GGT CAG GTG GGA TAG CGT TCC GCG TAT GGC CCA GCG CAT CAC GGG TTC GCA CCA-3′, were obtained from Sangon Biotechnology Co. Ltd. (www.sangon.com, Shanghai, China) and kept frozen at −20 °C for storage. $HAuCl_4 \cdot 4H_2O$, cysteamine hydrochloride and $NaBH_4$ were purchased from Sinopharm Chemical Reagent (Shanghai, China). BPA, 4,4′-bisphenol (BP), 2,2-bis(4-hydroxy-3-methylphenyl) propane (BPC), estriol, 17β-estradiol (ES) and diethylstilbestrol (DES) were purchased

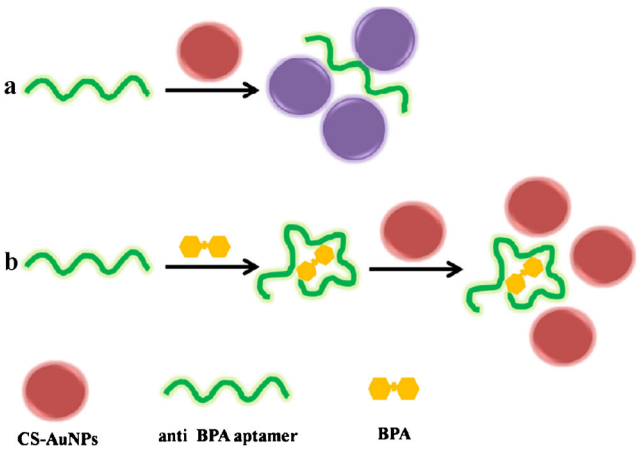

Scheme 1 Schematic illustration of the colorimetric aptasensor for the BPA detection using anti-BPA aptamers and cysteamine-AuNPs

from Sigma-Aldrich (http://www.sigmaaldrich.com/china-mainland.html, USA). 4-Tert-butylphenol (PTBP) and 3,3′,5,5′-tetrabromobisphenol A (TBBPA) were purchased from Aladdin Reagent Company (http://www.aladdin-e.com, Shanghai, China). All the chemicals were of analytical grade and were used without any further purification. Triply distilled water (TDW) was used throughout the experiments.

Apparatus

The absorption spectra were recorded on a 2550 UV-vis spectrophotometer (Shimadzu, Tokyo, Japan). Vortex mixing was performed on a WH-3 vortex mixer (Huxi, Shanghai, China). Transmission electron microscopy (TEM) measurements were made on a JEM-2100F (JEOL Co., Japan) operated at an accelerating voltage of 200 kV. Zeta potential (ζ) and dynamic light scattering (DLS) measurements were performed on a Nano ZS Laser Scattering Particles Size Analyzer (Malvern, England). The centrifugation was carried out on a CR20B2 refrigerated centrifuge (Tokyo, Japan). The circular dichroism (CD) spectral measurement was performed on a PMS 450 circular dichroism spectropolarimeter (BioLogic Science Instruments, France). The ultrasonic treatment was carried out on a 125 KQ-300DE ultrasonicator (Kunshan Ultrasonic Instrument Co., Shanghai, China). The photographs were taken with Casio EX-Z2300 digital camera.

Synthesis of cysteamine-AuNPs

All glassware used in the following procedure was cleaned in a bath of freshly prepared 3:1 HNO_3-HCl, rinsed thoroughly in water and dried fully prior to use. The positively-charged AuNPs were prepared by reducing $HAuCl_4$ with $NaBH_4$ in the presence of cysteamine [26]. Five hundred microliter of 213 mM cysteamine hydrochloride and 50 mL of 1.4 mM $HAuCl_4$ were stirring for 20 min at room temperature in the dark. Then 10 mM, 12.5 μL freshly prepared $NaBH_4$ was quickly added into the above mixure under vigorous stirring, and the mixture was further stirred for 30 min in the dark. The resulting wine-red solution was cysteamine-AuNPs solution and stored at 4 °C before use. The morphology and size distribution were characterized by TEM and DLS, and the average diameter of the AuNPs (39.5±1.3 nm) was measured by 140 nanoparticles on the TEM image using Nano Measurer 1.2.5. According to the Lambert-Beer law, the molar concentration of ~40 nm AuNPs was calculated to be 0.89 nM with the molar extinction coefficient of about 7.66×10^9 M^{-1} cm^{-1} [27].

Colorimetric detection of BPA

In a 1.5 mL centrufuge tube, 50 μL of anti-BPA aptamers (final concentration is 7 nM) was mixed with different concentration of BPA respectively. After the obtained mixture was vortex-mixed thoroughly and equilibrated for 12 min at room temperature, 0.125 nM of AuNPs solution was added into the above mixture and incubated at room temperature for further 12 min. Then the mixture was diluted to 500 μL with TDW. The absorption spectrum of the reacted solution was recorded with 1 cm path length cuvette. The calibration curve for BPA was established according to the absorbance ratio of A_{527}/A_{680} of the system.

Results and disscution

Principle of the aptamers-based colorimetric sensing for BPA using cysteamine-AuNPs as probe

This colorimetric sensing for BPA is based on the specific recognition between BPA and the anti-BPA aptamers. The specific binding between them was verified by circular dichroism (CD) spectroscopy. CD spectroscopy can measure the difference in the absorption of left and right circularly polarized light and is sensitive to the secondary structure of DNA, usually regarded as the most appropriate technique to distinguish different DNA structures [28]. As shown in Fig. S1 (Electronic Supplementary Material, ESM), the CD spectra of the pure aptamers before and after the binding of BPA were compared. In the absence of BPA, there was a positive band at ~280 nm and a negative band at ~240 nm (Fig. S1, curve a), which was respectively attributed to the base stacking interactions and the helicity [29]. It indicated that B-form structures primarily existed in the unbound anti-BPA aptamers. Upon the

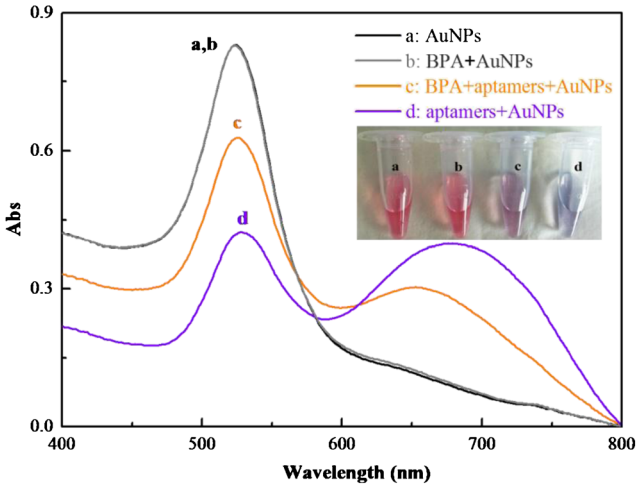

Fig. 1 Absorption spectra and visual observation (*Inset*) of cysteamine-AuNPs in different systems. **a** cysteamine-AuNPs; **b** cysteamine-AuNPs after addition of BPA; **c** cysteamine-AuNPs after addition of BPA and anti-BPA aptamers; **d** cysteamine-AuNPs after addition of anti-BPA aptamers. Cysteamine-AuNPs, 0.125 nM; anti-BPA aptamers, 7 nM; BPA, 100 $ng\cdot mL^{-1}$

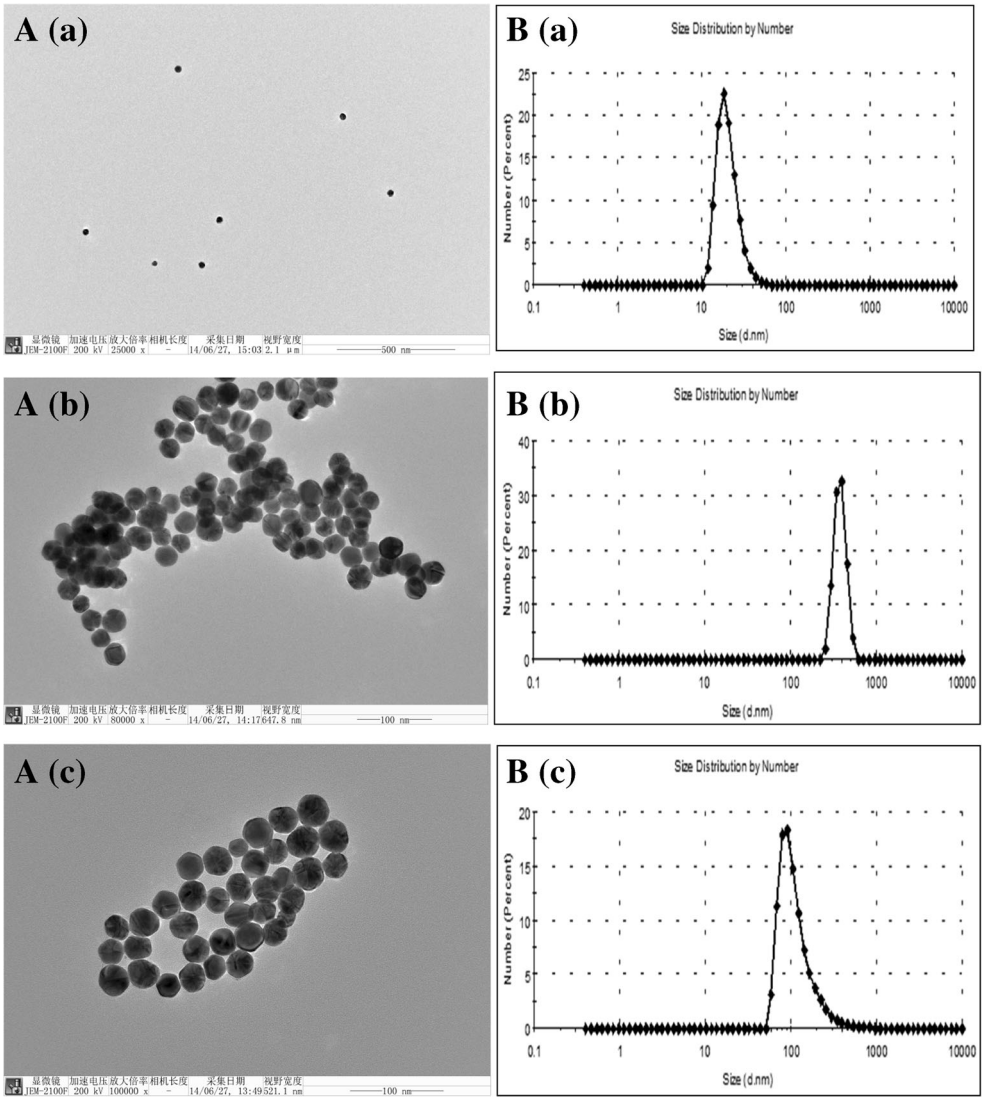

Fig. 2 TEM micrographs (**a**) and DLS images (**b**) of cysteamine-AuNPs in different systems. (**a**) cysteamine-AuNPs; (**b**) cysteamine-AuNPs after addition of anti-BPA aptamers; (**c**) cysteamine-AuNPs after addition of BPA and anti-BPA aptamers. Cysteamine-AuNPs, 0.125 nM; anti-BPA aptamers, 7 nM; BPA, 100 ng·mL^{-1}

addition of BPA, the amplitude of positive band around 280 nm and negative band around 240 nm increased without shift in the band positions (Fig. S1, curve b). This reveals that the addition of BPA can affect the base stacking and the right-handedness of aptamers [29], which causes the conformation change of anti-BPA aptamers. It is well known that the specific interaction between aptamers and the target requires the aptamers to adopt a unique folded structure to the target [30]. For small molecular targets, they tend to bury within the binding pockets of aptamers structure [31]. BPA can bind with the anti-BPA aptamers due to the strong affinity effects including the electrostatic effect, hydrogen bond effect, and spatial matching effect etc. [25], which leads the change of the anti-BPA aptamers configuration to pocket the BPA inside.

Cysteamine-AuNPs were prepared by reducing $HAuCl_4$ with $NaBH_4$ in the presence of cysteamine. During the synthetic process, cysteamine was capped onto the surfaces of the AuNPs through strong Au-S bonds, and the -NH_3^+ terminus of cysteamine imparted positive charges to the AuNPs, which was proved with the fact that the zeta potential of the cysteamine-AuNPs was + 16.2 mV (Fig. S2A, ESM)). Therefore, the cysteamine-AuNPs solution can be highly stabilized against aggregation due to the positive capping agent's electrostatic repulsion between AuNPs. The cysteamine-AuNPs were wine-red in color and showed an absorption peak at 527 nm, which was ascribed to the surface plasmon resonance of the AuNPs (Fig. 1, curve a). Upon addition of the anti-BPA aptamers into the positively-charged cysteamine-AuNPs, the characteristic absorption at 527 nm of cysteamine-AuNPs decreased significantly and the color of AuNPs solution changed to blue (Fig. 1, curve d). This is because that the negatively-charged backbones of the aptamers can facilitate cysteamine-AuNPs into close proximity with each other through electrostatic interaction, resulting in the aggregation of the AuNPs. The

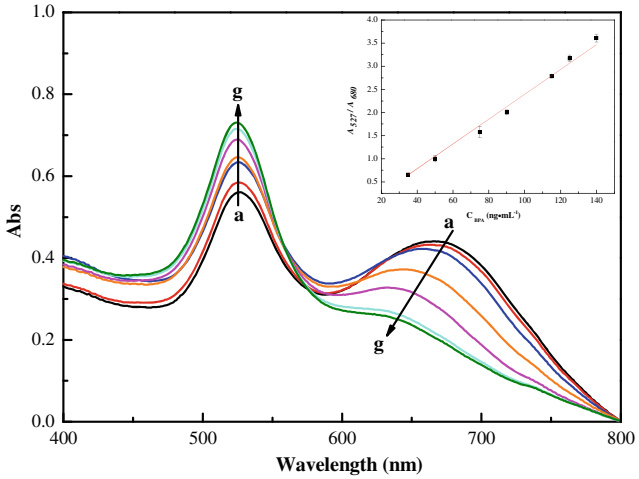

Fig. 3 Absorption spectra of the cysteamine-AuNPs when the aptasenor was utilized for different concentrations of BPA (35, 50, 75, 90, 115, 125, 140 ng·mL^{-1}) under the optimized experimental conditions. Inset: The linear calibration curve of A_{527}/A_{680} versus the concentration of BPA. Cysteamine-AuNPs, 0.125 nM; anti-BPA aptamers, 7 nM; incubation time of BPA and anti-BPA aptamers under vigorous stirring, 12 min; reaction time after addition of cysteamine-AuNPs into the incubation mixture of BPA and anti-BPA aptamers, 12 min

control experiment was performed using negatively-charged citrate-stabilized AuNPs (13 nm). The results (Fig. S3, ESM) showed that the aptamers do not aggregate the negatively-charged citrate-stabilized AuNPs, further confirming that the electrostatic attraction between cysteamine-AuNPs and the aptamers led to the aggregation of the cysteamine-AuNPs. However, in the presence of BPA, the anti-BPA aptamers can undergo folding by the induced fit binding mechanism and realize the structural conformation change, which prevents the aggregation of AuNPs. So the presence of BPA can eliminate the aptamers-induced spectral change and color transition of AuNPs (Fig. 1, curve c). Notably, it is found that without the presence of anti-BPA aptamers, the absorption spectrum of AuNPs was not affected by BPA (Fig. 1, curve b), suggesting that there was no interaction between BPA and AuNPs. The spectral changes of AuNPs in curve d and curve c were indeed induced by anti-BPA aptamers and the specific binding of aptamers with BPA.

The zeta potential of AuNPs in different system has also been measured. As mentioned above, the original cysteamine-AuNPs solution is positively charged (Fig. S2A). However, the zeta potential of AuNPs solution was −31.5 mV upon addition of anti-BPA aptamers (Fig. S2B, ESM). In the presence of BPA, the mixture showed the potential of +13.1 mV (Fig. S2C, ESM), suggesting that the strongly specific interactions between the BPA-binding aptamers and BPA can prevent the aggregation of cysteamine-AuNPs. Consequently, the AuNPs can maintain the dispersed and positively-charged state. The TEM and DLS characterization (Fig. 2) further confirm the principle of the colorimetric detection of BPA mediated by cysteamine-AuNPs. The original cysteamine-AuNPs were spherical in shape and well monodispersed with an average diameter of 39.5±1.3 nm (a). After interaction with anti-BPA aptamers, significant aggregation of AuNPs was observed (b). However, it can be observed that the specific binding of anti-BPA aptamers to BPA can prevent the aggregation of the cysteamine-AuNPs (c). These phenomena were consistent with the changes observed in the absorption spectra (Fig. 1). Consequently, the specific recognition between anti-BPA aptamers and BPA can induce the obvious changes in color and

Table 1 The comparison results of different methods for detection of BPA

Methods	Analytical range	LOD	Comments	Ref
LC-MS	0.45–90 ng·mL^{-1}	0.1 ng·mL^{-1}	Size-exclusion flow extraction	[3]
HPLC	0.5–200 ng·mL^{-1}	0.2 ng·mL^{-1}	Three-phase hollow fiber liquid-phase microextraction	[4]
GC-MS	–	1–5, 20, 100, and 20 pg·mL^{-1}	Stir bar sorptive extraction	[2]
Electrochemical sensor	50–2002 ng·mL^{-1}	8.644 ng·mL^{-1}	Mesoporous silica molecular sieves	[5]
Electrochemical sensor	2–700 ng·mL^{-1}	1.14 ng·mL^{-1}	PAMAM-Fe_3O_4 modified electrode	[6]
Electrochemical sensor	0.1–1000 pg·mL^{-1}	0.284 pg·mL^{-1}	Aptamer modified electrode	[32]
Immuno sensor	0–20 ng·mL^{-1}	5 and 0.92 ng·mL^{-1}	On-site detection; AuNPs labeled antibody	[33]
Immuno sensor	1.0 fg·mL^{-1}–1.0 ng·mL^{-1}	0.3 ng·mL^{-1}	Fluorescence immunoassay; Multi steps	[34]
ELISA	1.56 –100 ng·mL^{-1}	0.3 ng·mL^{-1}	Human colostrums; Time consuming	[7]
Fluorescent aptasensor	0.1–10 ng·mL^{-1}	0.05 ng·mL^{-1}	Fluorescently modified aptamer	[35]
Colorimetric aptasensor	0.11–10,000 ng·mL^{-1}	0.1 ng·mL^{-1}	Salt-induced (−)AuNPs aggregation	[18]
Colorimetric aptasensor	1–10,000 ng·mL^{-1}	0.1 ng·mL^{-1}	Salt-induced (−)AuNPs aggregation	[24]
Colorimetric aptasensor	35–140 ng·mL^{-1}	0.11 ng·mL^{-1}	Aptamers-induced (+)AuNPs aggregation	This method

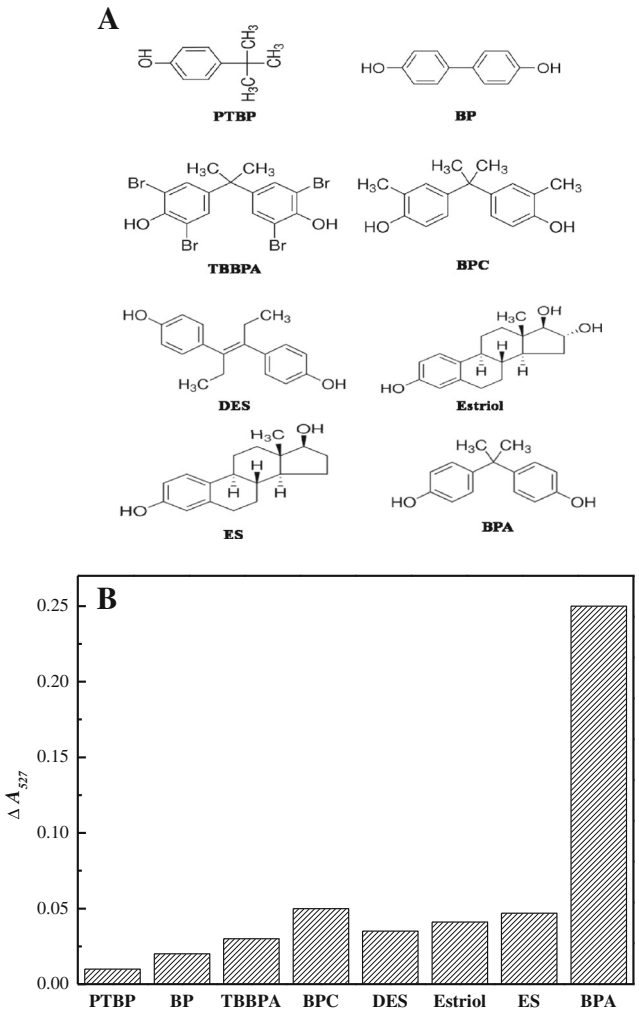

Fig. 4 **a** Chemical structures of BPA, TBBPA, BPC, BP, PTBP, Estriol, ES and DES; **b** The specificity testing results of the developed aptasensor

absorption properties of the cysteamine-AuNPs, based on which a simple colorimetric assay for BPA was developed in the present work.

Optimization of experimental conditions

The performance of the developed colorimetric assay is strongly influenced by the assay conditions. Thus the following parameters were optimized: (a) concentration of cysteamine-AuNPs, (b) concentration of anti-BPA aptamers, (c) the reaction time of cysteamine-AuNPs with anti-BPA aptamers, and (d) the binding time of BPA with its specific aptamers. Respective data and figures are given in the Electronic Supporting Material (Fig. S4). The following experimental conditions were found to give best results: (a) A cysteamine-AuNPs concentration of 0.125 nM (Fig. S4A), (b) a 7 nM concentration of anti-BPA aptamers (Fig. S4B), (c) a reaction time of 12 min (Fig. S4C), and (d) a binding time of 12 min (Fig. S4D).

Analytical performance and selectivity study

Then the established colorimetric method was applied for the determination of BPA. As presented in Fig. 3, the absorption spectral changes of cysteamine-AuNPs indicated that the aptamers-induced aggregation of cysteamine-AuNPs was gradually alleviated with the increasing concentration of BPA, accompanied with the gradual increase of A_{527} and the decrease of A_{680}. The absorbance ratio of A_{527}/A_{680} was linearly proportional to the concentration of BPA over the range of 35 to 140 ng·mL^{-1}, and the corresponding detection limit was calculated to be 0.11 ng·mL^{-1} (S/N=3). It should be noted that the detection limit of the developed method is much lower than the regulations for residues of BPA (50 ng·mL^{-1}) set by both the United States Federal Drug Administration (FDA) and China [18]. Furthermore, the specific features of this assay and other existing methods were compared and summarized in Table 1. It indicated that chromatographic techniques are sensitive and accurate. However, they have several disadvantages of time-consuming, complicated sample pretreatment and the need of expert personnel. The electrochemical aptasensor developed by Xue et al. [32] displays the excellent specificity and sensitivity. Accordingly, the fabrication of the electrode modified with aptamers needs complicated steps. Immunoassay-based methods have also attracted considerable attention for BPA detection due to the high sensitivity and comparable low costs of these techniques. However, they are strongly dependent on the quality of the prepared antibody, and the nonspecific binding to the analogs may give erroneous results. Currently, the existing colorimetric aptasensors for the detection of BPA are mainly based on the salt-induced aggregation of negatively-charged AuNPs [18, 24]. The aptamers can be adsorbed onto the negatively-charged AuNPs through the coordination interaction, thus maintain good tolerance of

Table 2 Determination of BPA in tap water spiked with different amounts of BPA by this colorimetric aptasensor and HPLC (n=3)

Sample	Amount added (ng·mL^{-1})	Amount found (ng·mL^{-1})		Recovery (%)±RSD (%)	
		This method	HPLC	This method	HPLC
1	80	72.96	89.95	91±3.52	112±9.30
2	110	116.60	110.84	106±2.20	101±6.18
3	160	155.96	161.35	97±2.19	101±4.43

AuNPs under aqueous conditions with high salt concentrations. In the presence of BPA, the AuNPs will aggregate due to the formation of BPA-aptamers complex. However, this method is susceptible to the sensing environments. Besides, the presence of salt solution makes the method more complicated. Obviously, this colorimetric aptasensor based on the positively-charged AuNPs is simple and rapid, but also presents a relatively competitive detection limit.

The specificity of the developed method was tested using seven kinds of analogues and the common environmental pollutants, including 4-tert-butylphenol (PTBP), 3,3′,5,5′-tetrabromobisphenol A (TBBPA), 4,4′-bisphenol (BP), 2,2-bis(4-hydroxy-3-methylphenyl) propane (BPC), estriol, 17β-estradiol (ES) and diethylstilbestrol (DES). The chemical structures of BPA and these compounds were shown in Fig. 4a. As illustrated in Fig. 4b, the established colorimetric method was used to detect BPA and these compounds, and only the interaction of BPA with anti-BPA aptamers can prevent the aptamers-induced aggregation of cysteamine-AuNPs and increase the A_{527}. The results indicated that the established assay is highly specific to BPA and has insignificant cross-reactivity with its analogues or common environmental pollutants. This remarkable specificity is attributed to the highly specific binding of anti-BPA aptamers to BPA.

Application to real samples

To further evaluate the performance and reliability of this aptasensor in practical applications, the spiked tap water samples were tested using the developed detection method. A known quantity of BPA was added into the tap water samples and diluted 20 times, then directly detected without any further pretreatments. Meanwhile, the spiked water samples were also analyzed by HPLC referenced in Chinese National Standard GB/T 23296.16-2009 (Food contact materials-polymer-determination of 2,2-bis (4-hydroxyphenyl) propane (bisphenol A) in food simulants-High performance liquid chromatography). The main experimental conditions of HPLC were shown as following: the chromatographic column used was C_{18} with the length of 250 mm and the inner diameter of 4.6 mm. The mobile phase was methanol and water (V:V=7:3), and the flow rate was 1 $mL \cdot min^{-1}$. The detector was fluorescence detector with the excitation wavelength of 227 nm and the emission wavelength of 313 nm. The data presented in Table 2 suggested that the results from the developed aptasensor were in full agreement with those from HPLC, which indicated that this method is highly reproducible and accurate for rapid screening of BPA. Obviously, this colorimetric aptasensor displayed the advantages of higher sensitivity and selectivity, handier operation and less detection time, which was commendably feasible for the rapid on-site BPA screening of real samples.

Conclusion

Using cysteamine-AuNPs as the probe and aptamers as the recognition element, a colorimetric aptasensor was successfully developed to detect BPA with the advantages of sensitivity, specificity and simplicity. The specific binding of BPA with the anti-BPA aptamers caused the conformation changes of aptamers, which can prevent the aptamers-induced aggregation and color change of cysteamine-AuNPs. Compared to previous colorimetric assays employing negatively-charged AuNPs as probe, this method is easy to perform because it avoids the procedure of salt-induced AuNPs aggregations. In addition, the direct "bare-eye" detection of BPA makes it more simple than other methods which mostly rely on advanced instrumentation. The method was successfully applied to detect BPA in tap water within 30 min, with the results in accordance with HPLC. In addition to these outstanding advantages of high selectivity and easy operation, this colorimetric aptasensor may be extended by using other aptamers for detecting environmental pollutants and harmful substances in food.

Acknowledgments This work was financially supported by the Natural Science Foundation of Jilin Province (No. 201215024), the Excellent Youth Talent Cultivation Project of Heping Campus of Jilin University, and the Graduate Student Innovation Research Project of Jilin University (No. 2014071).

References

1. Salian S, Doshi T, Vanage G (2011) Perinatal exposure of rats to bisphenol A affects fertility of male offspring-An overview. Reprod Toxicol 359–362
2. Kawaguchi M, Inoue K, Yoshimura M, Ito R, Sakui N, Okanouchi N, Nakazawa H (2004) Determination of bisphenol A in river water and body fluid samples by stir bar sorptive extraction with in situ derivatization and thermal desorption-gas chromatography-mass spectrometry. J Chromatogr B 805:41–48
3. Inoue K, Kawaguchi M, Funakoshi Y, Nakazawa H (2003) Size-exclusion flow extraction of bisphenol A in human urine for liquid chromatography-mass spectrometry. J Chromatogr B 798:17–23
4. Tan XW, Song YX, Wei RP, Yi GY (2012) Determination of trace bisphenol A in water using three-phase hollow fiber liquid-phase microextraction coupled with high performance liquid chromatography. Chin J Anal Chem 40:1409–1414
5. Wang FG, Yang JQ, Wu KB (2009) Mesoporous silica-based electrochemical sensor for sensitive determination of environmental hormone bisphenol A. Anal Chim Acta 638:23–28
6. Yin HS, Cui L, Chen QP, Shi WJ, Ai SY, Zhu LS, Lu LN (2011) Amperometric determination of bisphenol A in milk using PAMA M-Fe_3O_4 modified glassy carbon electrode. Food Chem 125:1097–1103
7. Kuruto-Niwa R, Tateoka Y, Usuki Y, Nozawa R (2007) Measurement of bisphenol A concentrations in human colostrums. Chemosphere 66:1160–1164
8. Ellington AD, Szostak JW (1990) In vitro selection of RNA molecules that bind specific ligands. Nature 346:818–822

9. Tuerk C, Gold L (1990) Systematic evolution of ligands by exponential enrichment: RNA ligands to bacteriophage T4 DNA polymerase. Science 249:505–510
10. Liu CW, Huang CC, Chang HT (2009) Highly selective DNA-based sensor for lead(II) and mercury(II) ions. Anal Chem 81: 2383–2387
11. Feng CJ, Dai S, Wang L (2014) Optical aptasensors for quantitative detection of small biomolecules: a review. Biosens Bioelectron 59: 64–74
12. Deng B, Lin YW, Wang C, Li F, Wang ZX, Zhang HQ, Li XF, Le XC (2014) Aptamer binding assays for proteins: the thrombin example-A review. Anal Chim Acta 837:1–15
13. Torres-Chavolla E, Alocilja EC (2009) Aptasensors for detection of microbial and viral pathogens. Biosens Bioelectron 24:3175–3182
14. Phillips JA, Lopez-Colon D, Zhu Z, Xu Y, Tan WH (2008) Applications of aptamers in cancer cell biology. Anal Chim Acta 621:101–108
15. Cho EJ, Lee JW, Ellington AD (2009) Applications of aptamers as sensors. Annu Rev Anal Chem 2:241–264
16. Chen XJ, Wang YZ, Zhang YY, Chen ZH, Liu Y, Li ZL, Li JH (2014) Sensitive electrochemical aptamer biosensor for dynamic cell surface N Glycan evaluation featuring multivalent recognition and signal amplification on a dendrimer−graphene electrode interface. Anal Chem 86:4278–4286
17. Liu CW, Hsieh YT, Huang CC, Lin ZH, Chang HT (2008) Detection of mercury(II) based on Hg^{2+}-DNA complexes inducing the aggregation of gold nanoparticles. Chem Commun 2242–2244
18. Mei ZL, Chu HQ, Chen W, Xue F, Liu J, Xu HN, Zhang R, Zheng L (2013) Ultrasensitive one-step rapid visual detection of bisphenol A in water samples by label-free aptasensor. Biosens Bioelectron 39: 26–30
19. Zheng Y, Wang Y, Yang XR (2011) Aptamer-based colorimetric biosensing of dopamine using unmodified gold nanoparticles. Sens Actuators B 156:95–99
20. Wei H, Li BL, Li J, Wang EK, Dong SJ (2007) Simple and sensitive aptamer-based colorimetric sensing of protein using unmodified gold nanoparticle probes. Chem Commun 36:3735–3737
21. Cao R, Li BX (2011) A simple and sensitive method for visual detection of heparin using positively-charged gold nanoparticles as colorimetric probes. Chem Commun 47:2865–2867
22. Cao R, Li BX, Zhang YF, Zhang ZN (2011) Naked-eye sensitive detection of nuclease activity using positively-charged gold nanoparticles as colorimetric probes. Chem Commun 47:12301–12303
23. Ren S, Li BX, Zhang L (2013) Visual detection of hexokinase activity and inhibition with positively charged gold nanoparticles as colorimetric probes. Analyst 138:3142–3145
24. Ragavan KV, Selvakumar LS, Thakur MS (2013) Functionalized aptamers as nano-bioprobes for ultrasensitive detection of bisphenol-A. Chem Commun 49:5960–5962
25. Jo M, Ahn JY, Lee J, Lee S, Hong SW, Yoo JW, Kang J, Dua P, Lee DK, Hong S (2011) Development of single-stranded DNA aptamers for specific bisphenol A detection. Oligonucleotides 21:85–91
26. Niidome T, Nakashima K, Takahashi H, Niidome Y (2004) Preparation of primary amine-modified gold nanoparticles and their transfection ability into cultivated cells. Chem Commun 17:1978–1979
27. Saha K, Agasti SS, Kim C, Li X, Rotello VM (2012) Gold nanoparticles in chemical and biological sensing. Chem Rev 112:2739–2779
28. Chang YM, Chen CKM, Hou MH (2012) Conformational changes in DNA upon ligand binding monitored by circular dichroism. Int J Mol Sci 13:3394–3413
29. Zhang ZL, Huang WM, Tang JL, Wang EK, Dong SJ (2002) Conformational transition of DNA induced by cationic lipid vesicle in acidic solution: spectroscopy investigation. Biophys Chem 97:7–16
30. Hermann T, Patel DJ (2000) Adaptive recognition by nucleic acid aptamers. Science 287:820–825
31. Kim YJ, Kim YS, Niazi JH, Gu MB (2010) Electrochemical aptasensor for tetracycline detection. Bioprocess Biosyst Eng 33: 31–37
32. Xue F, Wu JJ, Chu HQ, Mei ZL, Ye YK, Liu J, Zhang R, Peng CF, Zheng L, Chen W (2013) Electrochemical aptasensor for the determination of bisphenol A in drinking water. Microchim Acta 180: 109–115
33. Mei ZL, Deng Y, Chu HQ, Xue F, Zhong YH, Wu JJ, Yang H, Wang ZC, Zheng L, Chen W (2013) Immunochromatographic lateral flow strip for on-site detection of bisphenol A. Microchim Acta 180:279–285
34. Du LY, Zhang CY, Wang LJ, Liu GF, Zhang YF, Wang SH (2015) Ultrasensitive time-resolved microplate fluorescence immunoassay for bisphenol A using a system composed on gold nanoparticles and a europium(III)-labeled streptavidin tracer. Microchim Acta 182: 539–545
35. Zhu YY, Cai YL, Xu LG, Zheng LX, Wang LM, Qi B, Xu CL (2015) Building an aptamer/graphene oxide FRET biosensor for one-step detection of bisphenol A. ACS Appl Mater Interfaces 7: 7492–7496